High glucose induces HSP47 expression and promotes the secretion of inflammatory factors through the IRE1α/XBP1/HIF-1α pathway in retinal Müller cells

XINCHENG SUN[1,2], CHEN CHEN[2], HU LIU[1] and SHAOWEN TANG[3]

[1]Department of Ophthalmology, The First Affiliated Hospital of Nanjing Medical University,
Nanjing, Jiangsu 210029; [2]Department of Ophthalmology, The Affiliated Changzhou No.2 People's Hospital of
Nanjing Medical University, Changzhou, Jiangsu 213003; [3]Department of Epidemiology,
School of Public Health, Nanjing Medical University, Nanjing, Jiangsu 211166, P.R. China

Abstract. Diabetic retinopathy, a common complication of diabetes, is the leading cause of blindness globally. Müller cells are key players in diabetes-associated retinal inflammation and dysfunction. However, the pathological changes of Müller cells in response to high glucose (HG) and the underlying mechanism remain unclear. The aim of the present study was to investigate the key role of heat shock protein 47 (HSP47) in HG-induced unfolded protein and inflammatory responses. Primary mouse Müller cells were starved in serum-free DMEM overnight and then treated with HG (30 mM) for 0, 6, 12 or 24 h. It was observed that HG (30 mM) significantly induced the protein expression of HSP47, inositol-requiring transmembrane kinase and endonuclease-1α (IRE1α) and spliced X-box-binding protein 1 (XBP1s) in primary mouse Müller cells compared with the untreated group. In addition, the immunoprecipitation results revealed that HSP47 directly interacted with IRE1α, and this interaction was significantly enhanced by HG exposure for 12 or 24 h compared with the untreated group. Furthermore, small interfering RNA-mediated silencing of HSP47 significantly suppressed HG-induced activation of the IRE1α/XBP1s/hypoxia inducible factor-1 subunit α (HIF-1α) pathway and upregulation of the mRNA expression levels of the inflammatory cytokines vascular endothelial growth factor, platelet-derived growth factor subunit B, inducible nitric oxide synthase and angiopoietin-2 in Müller cells. Furthermore, overexpression of IRE1α or HIF-1α partially attenuated HSP47-siRNA-mediated inhibition of inflammatory cytokine expression in Müller cells. Collectively, these results indicated that HG may induce HSP47 expression and promote the inflammatory response through enhancing the interaction between HSP47 and IRE1α, and activating the IRE1α/XBP1s/HIF-1α pathway in retinal Müller cells.

Introduction

Diabetic retinopathy (DR), a common complication of diabetes, is the leading cause of vision impairment and blindness in the working-age population worldwide, displaying a continuous increase in incidence and prevalence over the past decades (1-3). Initially, DR was considered as a microvascular complication of diabetes and great efforts were made to develop strategies aimed at alleviating vascular alterations (3-5). However, due to the multifactorial etiology underlying the pathological process of DR, there is currently no effective treatment for restoring normal vision in patients. DR has been considered as a neurodegenerative disease, with an increasing number of studies reporting the contribution of retinal inflammation and glial cell activation to the development of DR (6,7). However, the molecular mechanisms underlying the retinal inflammation observed in response to high glucose (HG) remain to be elucidated.

Müller cells, the most abundant type of glial cells in the retina, serve a fundamental role in maintaining the blood-retinal barrier, controlling the metabolism of nutrients and supporting the function of retinal neurons (8,9). Müller cells are activated in DR, which is characterized by increased expression of glial fibrillary acidic protein and the release of inflammatory cytokines and chemokines (8,10,11). Thus, elucidating the mechanism underlying the response of Müller cells to HG may uncover new therapeutic targets for DR. The release of growth factors and pro/anti-inflammatory cytokines, mitochondrial dysfunction and endoplasmic reticulum (ER)

Correspondence to: Professor Hu Liu, Department of Ophthalmology, The First Affiliated Hospital of Nanjing Medical University, 300 Guangzhou Road, Nanjing, Jiangsu 210029, P.R. China
E-mail: liuhueye@163.com

Professor Shaowen Tang, Department of Epidemiology, School of Public Health, Nanjing Medical University, 101 Longmian Road, Nanjing, Jiangsu 211166, P.R. China
E-mail: tomswen@njmu.edu.cn

stress in HG-induced Müller cells have been implicated in the pathogenesis of DR (12-14).

Heat shock protein 47 (HSP47), which is encoded by the serpin family H member 1 gene, is a collagen-specific molecular chaperone localized in the ER (15). HSP47 interacts with procollagen in the ER, which is essential for the folding and secretion of collagen proteins (15). Increased HSP47 expression has been reported in numerous types of cancer, including squamous cell carcinoma of the lung and bronchial epithelium and gastric cancer (16,17), serving a role in cancer cell invasion and extracellular matrix network regulation (18). Sepulveda *et al* (19) revealed a novel role for HSP47 in unfolded protein response (UPR) regulation via directly binding with inositol-requiring transmembrane kinase and endonuclease-1α (IRE1α). Moreover, HSP47 was shown to trigger IRE1α activation, thereby inducing ER stress arising from protein synthesis under stress-induced tumor environment conditions (20). IRE1α is a sensor of unfolded protein accumulation in the ER that triggers the UPR. Once activated, IRE1α splices 26 nucleotides from X-box-binding protein 1 (XBP1) mRNA, leading to the generation of spliced XBP1 (XBP1s), which subsequently translocates to the nucleus and activates transcription of responsive genes (21). XBP1s forms a transcriptional complex with hypoxia-inducible factor-1 subunit α (HIF-1α), thereby regulating the expression of HIF-1α targets via recruiting RNA polymerase II (22). ER stress has been implicated in HG-induced Müller cell injury and inflammasome activation in DR (23). However, the role of the HSP47/IRE1α/XBP1s/HIF-1α pathway in the inflammatory response of Müller cells in DR remains elusive.

The present study aimed to investigate the effects of HSP47 and the UPR transducer IRE1α/XBP1s pathway on HG-induced mouse retinal Müller cells. Moreover, whether the effects of HSP47 on the expression of inflammatory cytokines in HG-exposed Müller cells were mediated through the IRE1α/XBP1s/HIF-1α pathway was investigated. In addition, the effects of HG on the expression of HSP47 and the interaction between HSP47 and IRE1α in Müller cells were assessed. Furthermore, the effects of HSP47 on the activation of the IRE1α/XBP1s/HIF-1α pathway and the expression of inflammatory cytokines were assessed following HSP47 silencing. Collectively, the aim of the present study was to identify novel therapeutic targets for alleviating the pathogenesis of DR.

Materials and methods

Mouse retinal Müller cell culture. Mouse retinal Müller cells were isolated from C57BL/6 mice as previously described (24). The mice [n=20; weight, 3-5 g; sex, male (n=10) and female (n=10); age, 7-10-day-old] were purchased from Charles River Laboratories (Beijing, China). After receiving them, the mice were immediately euthanized by CO_2 asphyxiation, with a CO_2 displacement rate of 20% of the chamber volume per min. After confirming animal death by observing reduced body temperature and pale skin, the eyes were enucleated and washed in PBS containing penicillin (100 U/ml; Thermo Fisher Scientific, Inc.) and streptomycin (100 μg/ml; Thermo Fisher Scientific, Inc.). The retinas were then carefully isolated from the eyeballs and washed in PBS to avoid contamination with retinal pigment epithelium. Isolated retinas were cut

onto small pieces (1 mm) using micro scissors and gently dissociated using a sterile Pasteur pipette. The cell aggregates were centrifuged for 5 min at 896 x g at room temperature, and resuspended in DMEM (Thermo Fisher Scientific, Inc.) supplemented with 10% fetal bovine serum (Thermo Fisher Scientific, Inc.), 5 mM glucose and antibiotic mixture. Müller cells were plated ($5x10^5$) in a gelatin-coated dish and maintained at 37˚C in a humidified atmosphere with 5% CO_2. The culture medium was changed every 4-5 days and cells were passaged biweekly at a ratio of 1:3. Müller cells were identified by their characteristic bipolar morphology and immunostained with glutamine synthetase and glial fibrillary acidic protein (data not shown) (25). The purity of Müller cells was >90% after 2-3 passages. For the HG experiments, retinal Müller cells were starved in serum-free DMEM overnight and then treated with HG (30 mM) for 0, 6, 12 or 24 h. All animal experimental procedures were approved by the Ethics Committee for Laboratory Animals of the Nanjing Medical University (approval no. 20181207). The date of the original ethics approval was prior to 2020.

Cell transfection. The small interfering (si)RNA of HSP47 (HSP47-siRNA sense, 5'-GUUCCACCAUAAGAUGGUAGA CAACAG-3'; and antisense, 5'-GUUGUCUACCAUCUUAUG GUGGAACAU-3') and scrambled control siRNA (con-siRNA sense, 5'-CGAUUCGCUAGACCGGCUUCA UUGCAG-3'; and antisense, 5'-GCAAUGAAGCCGGUCUAGCGAAUCG AU-3') were provided by Sigma-Aldrich (Merck KGaA) and were transfected into cells (20 nmol/l) by Oligofectamine™ for 48 h (total volume, 20 μl; room temperature) following the manufacturer's protocol (Invitrogen; Thermo Fisher Scientific, Inc.). At 48 h post-transfection, transfection efficiency was determined via western blotting. Subsequent experiments were also performed at 48 h post-transfection. A total of 1 μl of a 20 μM stock oligonucleotide was diluted in 16 μl of Opti-MEM® I Reduced Serum Medium (Thermo Fisher Scientific, Inc.). The mix was added to cells ($5x10^5$) for 5-10 min at room temperature. HA-IRE1α and HA-HIF-1α were purchased from Addgene. The genes encoding IRE1α and HIF-1α were cloned into a pcDNA3 vector (Invitrogen; Thermo Fisher Scientific, Inc.) with the hemagglutinin tag. siRNAs and recombinant plasmids were electroporated into retinal Müller cells. Briefly, $5x10^5$ cells were resuspended in PBS 0.1X and gently mixed with the appropriate volume of siRNA (10 nM) in a final volume of 400 μl into 0.4 cm electroporation cuvettes. Cells were electroporated with two pulses of 850 V and 25 μF using a Biorad Gene Pulser II (Bio-Rad Laboratories, Inc.) apparatus and plated in DMEM medium supplemented with Geneticin™ Selective Antibiotic (G418 Sulfate; cat. no. 10131027; Thermo Fisher Scientific, Inc.) at a concentration of 800 μg/ml for 2 h at 37˚C, then cultured in DMEM medium supplemented with Geneticin™ Selective Antibiotic at a concentration of 800 μg/ml containing 20 mM NH_4Cl at 28˚C overnight. A scrambled siRNA and empty pcDNA3 vector were used as controls. At 48 h post-electroporation, transfection efficiency was determined via western blotting.

Reverse transcription-quantitative PCR (RT-qPCR). Cells were exposed to HG for 12 h prior to assessment via RT-qPCR.

Table I. Sequences of primers used for RT-qPCR.

Gene	Primer sequences (5' to 3')
HSP47	Forward: AAGATGGTAGACAACCGTGG
	Reverse: GTCTCGCATCTTGTCTCCCTT
IRE1α	Forward: GTGGTCTCCTCTCGGGTTC
	Reverse: CCGTCCCAGGTAGACACAAAC
XBP1s	Forward: AGCAGCAAGTGGTGGATTTG
	Reverse: GAGTTTTCTCCCGTAAAAGCTGA
VEGF	Forward: GAGGTCAAGGCTTTTGAAGGC
	Reverse: CTGTCCTGGTATTGAGGGTGG
PDGF-B	Forward: CATCCGCTCCTTTGATGATCTT
	Reverse: GTGCTCGGGTCATGTTCAAGT
iNOS	Forward: TCATGACATCGACCAGAAGC
	Reverse: GGACATCAAAGGTCTCACAG
ANGPT-2	Forward: CCTCGACTACGACGACTCAGT
	Reverse: TCTGCACCACATTCTGTTGGA
β-actin	Forward: GGCTGTATTCCCCTCCATCG
	Reverse: CCAGTTGGTAACAATGCCATGT

RT-qPCR, reverse transcription-quantitative PCR; HSP47, heat shock protein 47; IRE1α, inositol-requiring transmembrane kinase and endonuclease-1α; XBP1s, spliced X-box-binding protein 1; VEGF, vascular endothelial growth factor; PDGF-B, platelet-derived growth factor subunit B; iNOS, inducible nitric oxide synthase; ANGPT-2, angiopoietin 2.

The total RNA of Müller cells was extracted using TRIzol® (Thermo Fisher Scientific, Inc.). Total RNA was reverse transcribed into cDNA using the PrimeScript RT Reagent Kit with gDNA Eraser (Takara Bio, Inc.) following the manufacturer's protocol. The relative mRNA expression levels of HSP47, IRE1α, XBP1s, vascular endothelial growth factor (VEGF), platelet-derived growth factor subunit B (PDGF-B), inducible nitric oxide synthase (iNOS) and angiopoietin 2 (ANGPT-2) were measured via qPCR using SYBR Green qPCR Master Mix (Takara Bio, Inc.) on a 7500 Real-Time PCR system (Applied Biosystems; Thermo Fisher Scientific, Inc.). The thermocycling conditions were as follows: 10 min initial denaturation at 95°C; 40 cycles of 15 sec denaturation (95°C), 20 sec annealing (56°C) and 20 sec extension (72°C). At the end of each run, the instrument was set at 15 sec at 95°C, 60 sec at 60°C (melt curves analysis) and the final temperature was 95°C with 0.1°C/sec slope. Fold changes were calculated using the $2^{-\Delta\Delta Cq}$ method (26) using β-actin as the reference gene. The sequences of the primers used for qPCR are listed in Table I.

Western blotting, antibodies and reagents. Retinal Müller cells were harvested, washed with ice-cold PBS and lysed with 1X RIPA lysis buffer (Cell Signaling Technology, Inc.) on ice for 30 min. The protein concentration was determined using the BCA assay (Thermo Fisher Scientific, Inc.). The proteins (10 µg per lane) were separated via 10% SDS-PAGE gel (EpiZyme, Inc.) and transferred to a PVDF membrane (Merck KGaA). After blocking with 5% non-fat milk in TBST (200 mM Tris and 1.5 M NaCl with 0.1% Tween 20) for 2 h at room temperature, the membranes were incubated with the following primary antibodies at 4°C overnight:

Anti-HSP47 [1:800; mouse monoclonal antibody (mAb); cat. no. NBP1-97491; Novus Biologicals, LLC], anti-IRE1α (1:1,000; rabbit mAb; cat. no. 3294; Cell Signaling Technology, Inc.), anti-XBP1s (1:500; rabbit mAb; cat. no. 40435; Cell Signaling Technology, Inc.), anti-HIF-1α (1:800; rabbit mAb; cat. no. 36169; Cell Signaling Technology, Inc.) and GAPDH (1:2,000; rabbit polyclonal antibody; cat. no. AC027; ABclonal Biotech Co., Ltd.). The membranes were sequentially probed with a horseradish peroxidase-conjugated goat anti-rabbit IgG (1:2,000; cat. no. AS014; ABclonal Biotech Co., Ltd.) or goat anti-mouse IgG (1:2,000; cat. no. AS003; ABclonal Biotech Co., Ltd.) secondary antibody. GAPDH served as the loading control. Protein bands were visualized using the enhanced chemiluminescence substrate kit (Thermo Fisher Scientific, Inc.). ImageJ v1.8.0 (National Institutes of Health) was used for densitometry.

Immunoprecipitation. Mouse retinal Müller cells (5×10^6) were harvested and lysed in 100 µl immunoprecipitation lysis buffer (Thermo Fisher Scientific, Inc.) with proteinase/phosphatase inhibitor (Roche Diagnostics) for 1 h on ice. The lysis solution was centrifuged at 16,000 x g for 10 min at 4°C. The protein concentration of the lysis supernatants was determined using BCA assays (Thermo Fisher Scientific, Inc.) and adjusted to 1 mg/ml with lysis buffer. Samples were then incubated with an anti-HSP47 (1:50; mAb; cat. no. NBP1-97491; Novus Biologicals, LLC) or mouse IgG (1:500; rabbit mAb; cat. no. 5946; Cell Signaling Technology, Inc.) antibody overnight (12-16 h) in a 4°C fridge with gentle orbital rotation (7 x g). Subsequently, 50 µl of Protein Magnetic beads (Thermo Fisher Scientific, Inc.) were added into samples and incubated for another 12 h at 4°C. After incubation, the magnetic beads were centrifuged at 3,000 x g for 2 min, washed three times with ice-cold PBS and the supernatant was discarded. The proteins were eluted using 1X SDS protein gel sample loading buffer and subjected to western blotting according to the aforementioned protocol.

Statistical analysis. Each experiment in the present study was performed at least in triplicate. All data are presented as the mean ± SD. GraphPad Prism software v. 8.0.1 (GraphPad Software, Inc.) was used to perform all statistical analyses. Differences between multiple groups were analyzed using one-way or two-way ANOVA followed by Bonferroni's post hoc test. P-values were two-tailed and $P < 0.05$ was considered to indicate a statistically significant difference.

Results

HG exposure increases HSP47 expression in retinal Müller cells. To investigate the expression and function of HSP47, retinal Müller cells were isolated from C57BL/6 mice and cultured *in vitro*. The cells were treated with 30 mM glucose for 0, 6, 12 or 24 h, and the protein and mRNA expression levels of HSP47 were detected via western blotting and RT-qPCR, respectively. Compared with the untreated group, the protein expression level of HSP47 was significantly increased in Müller cells after exposure to HG, reaching the highest level at 12 h, with a slight decrease at a 24 h compared with 12 h (Fig. 1A and B). Therefore, treatment with HG for
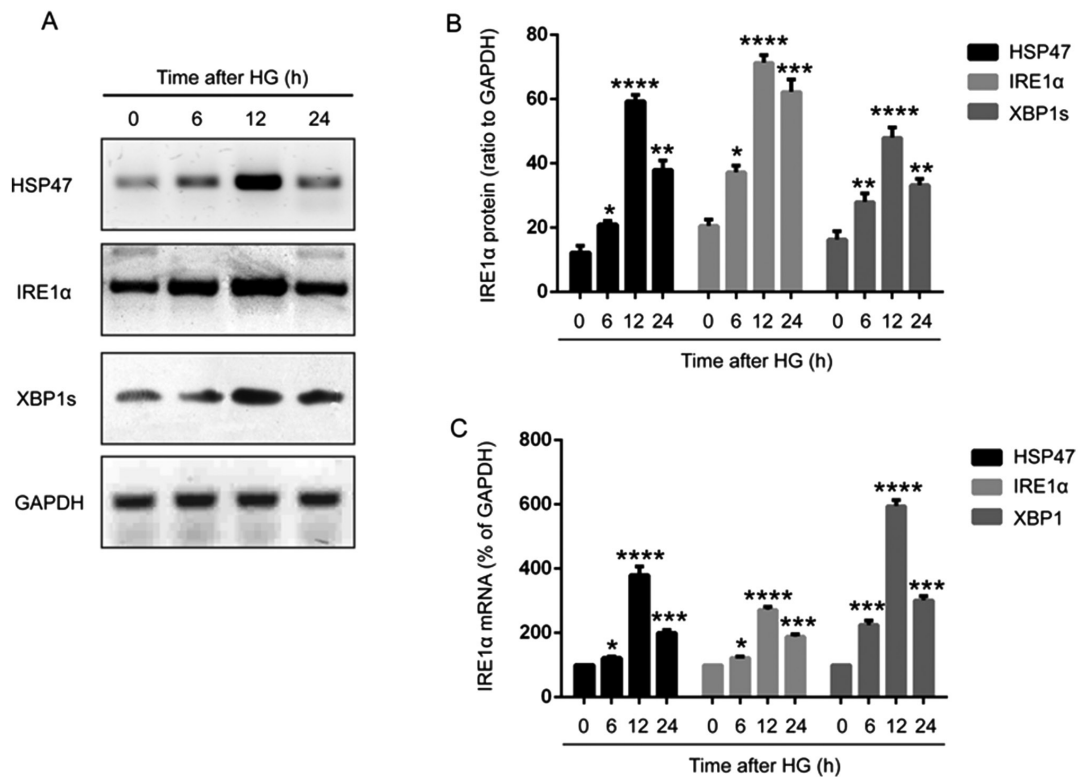
Figure 1. HG induces HSP47 expression in retinal Müller cells. Protein expression levels of HSP47, IRE1α and XBP1s in retinal Müller cells following exposure to HG (30 mM) for 0, 6, 12 or 24 h were (A) determined via western blotting and (B) semi-quantified. (C) Relative mRNA expression levels of HSP47, IRE1α and XBP1s in retinal Müller cells were determined via reverse transcription-quantitative PCR. Data are presented as the mean ± SD (n=3). Comparisons among multiple groups were analyzed using one-way ANOVA followed by Tukey's post hoc test. *P<0.05, **P<0.01, ***P<0.001 and ****P<0.0001 vs. 0 h. HG, high glucose; HSP47, heat shock protein 47; IRE1α, inositol-requiring transmembrane kinase and endonuclease-1α; XBP1s, spliced X-box-binding protein 1.
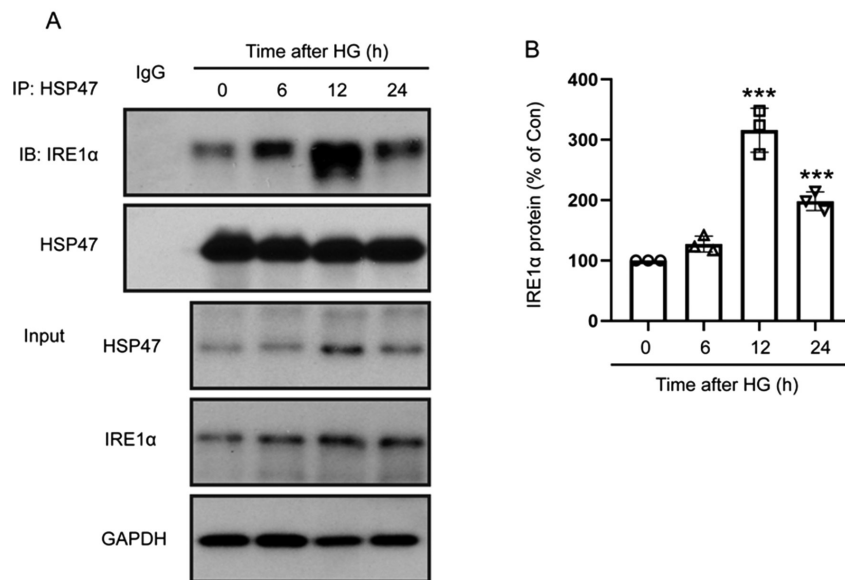

Figure 2. HG enhances the binding of HSP47 and IRE1α. (A) The interaction between HSP47 and IRE1α in retinal Müller cells was assessed by performing immunoprecipitation following exposure to HG (30 mM) for 0, 6, 12 or 24 h. The HSP47/IRE1α complex was immunoprecipitated using an anti-HSP47 antibody and assessed via western blotting using anti-IRE1α and anti-HSP47 antibodies. (B) Relative protein expression level of IRE1α was normalized to HSP47. Data are presented as the mean ± SD (n=3). The circle, triangle (up arrow), square and triangle (down arrow) represent 0, 6, 12 or 24 h after HG exposure, respectively. Comparisons among multiple groups were analyzed using one-way ANOVA followed by Tukey's post hoc test. ***P<0.001 vs. 0 h. HG, high glucose; HSP47, heat shock protein 47; IRE1α, inositol-requiring transmembrane kinase and endonuclease-1α.

12 h was selected for subsequent experiments. As expected, a similar trend was observed for HSP47 mRNA expression levels (Fig. 1C).

HG induces UPR in retinal Müller cells. To further examine whether IRE1α was involved in the effect of HSP47 on retinal Müller cells, the activation of the IRE1α/XBP1s pathway was
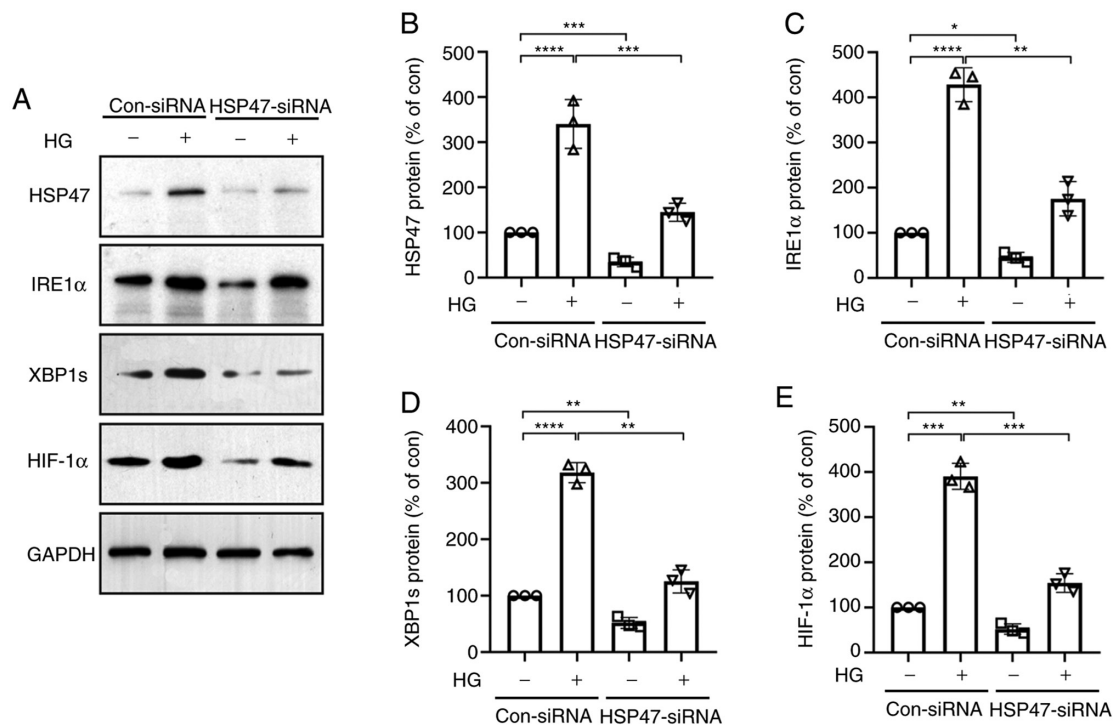
Figure 3. HG activates the IRE1α/XBP1s/HIF-1α pathway via HSP47. Retinal Müller cells were electroporated with con-siRNA or HSP47-siRNA. At 48 h post-electroporation, cells were exposed to HG (30 mM) for 12 h. (A) Protein expression levels of HSP47, IRE1α, XBP1s and HIF-1α in retinal Müller cells were (A) determined via western blotting and semi-quantified for (B) HSP47, (C) IRE1α, (D) XBP1s and (E) HIF-1α. Data are presented as the mean ± SD (n=3). The circle, triangle (up arrow), square and triangle (down arrow) represented con-siRNA without HG exposure, con-siRNA with HG exposure, HSP47-siRNA without HG exposure and HSP47-siRNA with HG exposure, respectively. Comparisons among multiple groups were analyzed using two-way ANOVA followed by Bonferroni's post hoc test. $^*P<0.05$, $^{**}P<0.01$, $^{***}P<0.001$ and $^{****}P<0.0001$. HG, high glucose; HSP47, heat shock protein 47; IRE1α, inositol-requiring transmembrane kinase and endonuclease-1α; XBP1s, spliced X-box-binding protein 1; HIF-1α, hypoxia inducible factor-1 subunit α; siRNA, small interfering RNA; con, control.

examined. The expression of IRE1α and XBP1s was significantly increased in HG-treated Müller cells (6, 12 and 24 h) compared with untreated cells, exhibiting a similar trend to HSP47 (Fig. 1A-C). Immunoprecipitation was then performed to determine the interaction between HSP47 and IRE1α, and the data revealed that HSP47 could bind directly to IRE1α in Müller cells, which was significantly enhanced when cells were treated with HG for 12 or 24 h compared with the untreated group (Fig. 2A and B). These results indicated that HG-induced activation of the IRE1α/XBP1s pathway in the retinal Müller cells was regulated by HSP47.

HG activates the IRE1α/XBP1s/HIF-1α pathway in retinal Müller cells through HSP47. To determine the exact role of HSP47 in regulating IRE1α and its downstream pathways, HSP47 was silenced in Müller cells via siRNA transfection. At 48 h post-electroporation of HSP47-siRNA or con-siRNA, Müller cells were exposed to HG for 12 h, and the protein expression levels of HSP47, IRE1α, XBP1s and HIF-1α were measured via western blotting. The expression levels of HSP47, IRE1α, XBP1s and HIF-1α were significantly decreased in the HSP47-siRNA group compared with the con-siRNA group without HG treatment (Fig. 3). The decrease in HSP47 in untreated retinal Müller cells, led to the suppression of IRE1α, XBP1s and HIF-1α expression (Fig. 3). In con-siRNA-transfected cells, the expression levels of HSP47, IRE1α, XBP1s and HIF-1α were significantly enhanced by HG compared with the untreated group (Fig. 3A-E). Interestingly,

HG-induced increases in IRE1α, XBP1s and HIF-1α expression levels were suppressed in HSP47-silenced Müller cells (Fig. 3A-E). These results indicated that HSP47 served a key role in IRE1α/XBP1s/HIF-1α pathway activation in HG-induced retinal Müller cells.

HSP47 regulates the expression of inflammatory mediators in retinal Müller cells through the IRE1α/XBP1s/HIF-1α pathway. It is well established that HG exposure leads to the high expression of inflammatory mediators in Müller cells, further contributing to the development of DR (8,27,28). As shown in Fig. 4, compared with the untreated group, the expression levels of VEGF, PDGF-B, iNOS and ANGPT-2 were significantly increased in HG-treated Müller cells, which was significantly attenuated in HSP47-silenced Müller cells. Transfection efficiencies of the IRE1α and HIF-1α overexpression vectors are presented in Fig. S1. Overexpression of IRE1α or HIF-1α partially reversed the inhibitory effects of HSP47-siRNA, resulting in significantly increased expression levels of VEGF, PDGF-B, iNOS and ANGPT-2 compared with the HSP47-siRNA group. These results demonstrated the effect of HSP47 on the IRE1α/XBP1/HIF-1α pathway and its involvement in the HG-induced inflammatory response in retinal Müller cells.

Discussion

The results of numerous studies have demonstrated the occurrence of inflammation in the retinas of diabetic animal
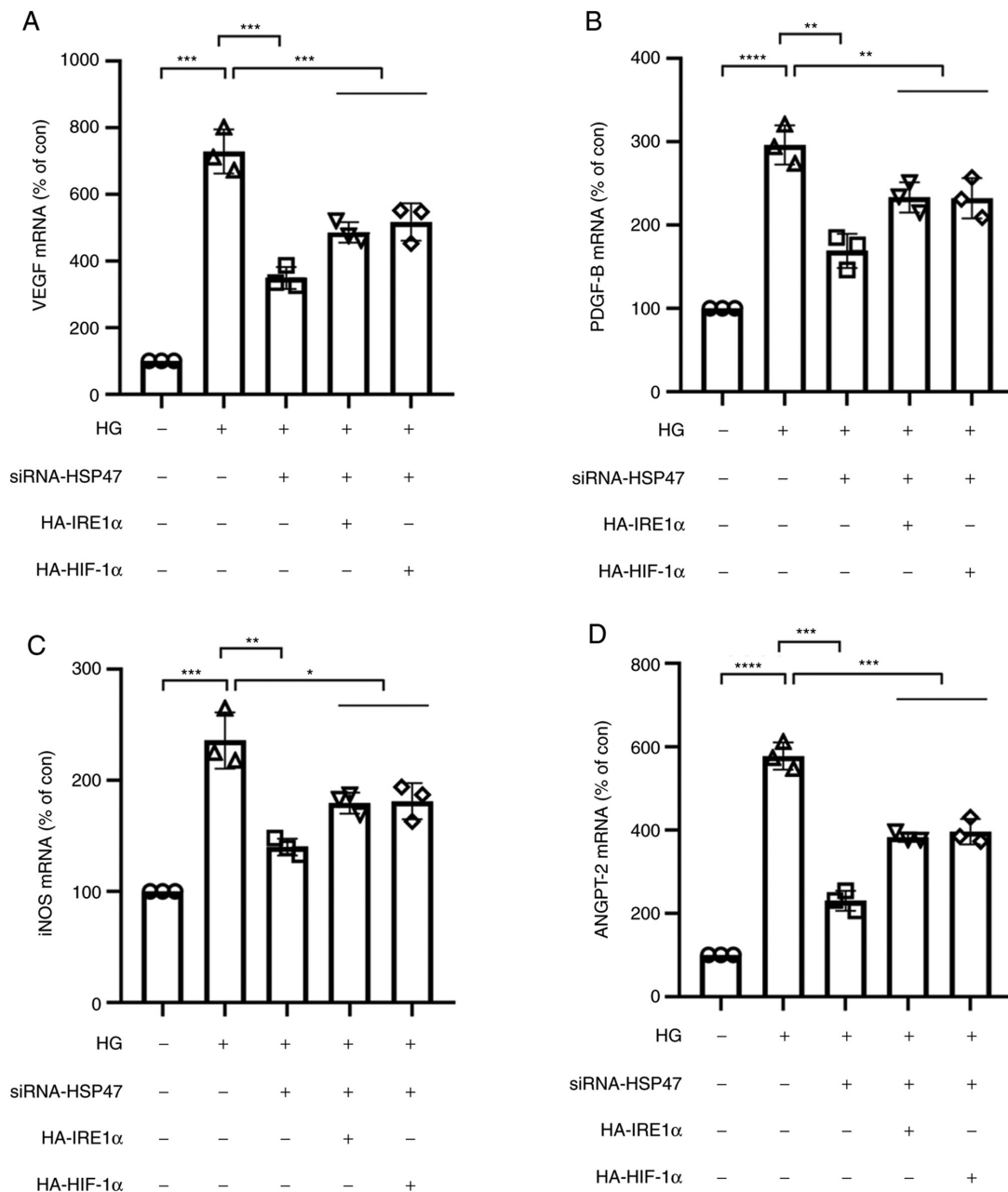
Figure 4. Expression of inflammatory cytokines in HSP47-silenced retinal Müller cells. Retinal Müller cells were transfected with HSP47-siRNA, HA-IRE1α or HA-HIF-1α plasmid. At 48 h post-transfection, retinal Müller cells were exposed to HG (30 mM) for 12 h, and the relative mRNA expression levels of (A) VEGF, (B) PDGF-B, (C) iNOS and (D) ANGPT-2 were measured via reverse transcription-quantitative PCR. Data are presented as the mean ± SD (n=3). The circle, triangle (up arrow), square, triangle (down arrow) and lozenge represent con-siRNA without HG exposure, con-siRNA with HG exposure, HSP47-siRNA with HG exposure, HSP47-siRNA with HG exposure and HA-IRE1α, and HSP47-siRNA with HG exposure and HA-HIF-1α, respectively. Comparisons among multiple groups were analyzed using one-way ANOVA followed by Bonferroni's post hoc test. *P<0.05, **P<0.01, ***P<0.001 and ****P<0.0001. HG, high glucose; HSP47, heat shock protein 47; siRNA, small interfering RNA; IRE1α, inositol-requiring transmembrane kinase and endonuclease-1α; HIF-1α, hypoxia inducible factor-1 subunit α; VEGF, vascular endothelial growth factor; PDGF-B, platelet-derived growth factor subunit B; iNOS, inducible nitric oxide synthase; ANGPT-2, angiopoietin 2; HA, hemagglutinin; con, control.

models and suggested the contribution of Müller cell activation to neovascularization and fibrosis during the progression of DR (8,29,30). As a subset of retinal innate immune cells, Müller cells maintain the nutrition of the retina through ion channels, ligand receptors and transmembrane transporters. High blood glucose levels and the leakage of retinal vessels leads to the activation and dysfunction of Müller cells (8,29,30). Several pathological changes in Müller cells are associated with the progression of DR, including abnormal regulation of neurotransmitters and potassium, release of growth factors

and pro/anti-inflammatory cytokines, and the loss of Müller cells (31,32). To the best of our knowledge, the present study was the first to demonstrate the critical role of HSP47 in the regulation of inflammatory mediator levels in HG-exposed retinal Müller cells through the IRE1α/XBP1/HIF-1α pathway using mouse primary Müller cells.

ER stress is a common pathological pathway in a number of ophthalmic diseases, such as DR, glaucoma, cataract and macular degeneration (33-36). The findings of the present study demonstrated that HG triggered ER stress as indicated

by increased expression of IRE1α and XBP1s compared with the untreated group. This result was consistent with the study conducted by Zhong *et al* (27) who reported that HG induced a time-dependent increase in ER stress in Müller cells and was essential for Müller cell-derived cytokine production in diabetes. Sepulveda *et al* (19) identified HSP47 as a novel selective regulator of the ER stress transducer IRE1α in mouse embryonic fibroblasts, but the mechanism underlying HSP47-mediated regulation of the IRE1α pathway remains unknown. The present study demonstrated that HG significantly induced the expression of the procollagen-interacting protein HSP47 in Müller cells compared with the untreated group, and the interaction between HSP47 and IRE1α was also enhanced by HG exposure, suggesting the regulatory effect of HSP47 on the IRE1α pathway and involvement of ER stress in HG-induced Müller cell activation. The expression of HSP47 decreased following treatment with HG for 24 h compared with treatment for 12 h, indicating that HSP47 and the downstream pathway were not continuously activated in response to HG due to adaptive or compensatory events.

Considering the direct modulatory effect of HSP47 on the IRE1α pathway, HSP47 was silenced by siRNA transfection to further investigate the exact mechanism underlying HSP47-mediated regulation of the inflammation of Müller cells in response to HG. The increase in the expression levels of IRE1α, XBP1s and HIF-1α induced by HG was significantly suppressed in HSP47-silenced Müller cells, suggesting the key role of HSP47 in IRE1α/XBP1/HIF-1α pathway activation. Furthermore, the increase in the expression levels of growth factors and inflammatory cytokines, including VEGF, PDGF-B, iNOS and ANGPT-2, induced by HG was significantly alleviated following HSP47 silencing. Overexpression of IRE1α or HIF-1α reversed the inhibitory effect of HSP47 silencing on expression, as demonstrated by significantly upregulated expression levels of inflammatory mediators in cells co-transfected with IRE1α or HIF-1α overexpression vectors compared with cells transfected with HSP47-siRNA alone. These data indicated that HG induced HSP47 expression and promoted the inflammatory response through enhancing the interaction between HSP47/IRE1α and activating the IRE1α/XBP1/HIF-1α pathway in retinal Müller cells. This may not be the only role of HSP47 in DR Müller cells as other pathological changes in DR, such as mitochondrial dysfunction and Müller cell apoptosis, may also be affected by HSP47 expression. As the present study was performed in cultured Müller cells *in vitro*, the role of HSP47 in DR Müller cells requires confirmation by performing further animal experiments and analyzing clinical data from patients.

In summary, the data of the present study demonstrated that exposure to HG induced HSP47 expression in Müller cells, leading to the activation of the IRE1α/XBP1/HIF-1α pathway and the production of inflammatory mediators via interacting with IRE1α. Thus, identifying novel therapeutic targets to alleviate the HSP47/IRE1α interaction and ER stress in Müller cells may prove helpful in preventing the pathogenesis of DR.

Availability of data and materials

The datasets used and/or analyzed during the current study are available from the corresponding author on reasonable request.

Authors' contributions

HL and ST designed the present study. XS and CC performed the experiments. HL and ST confirmed the authenticity of all the raw data. XS and CC drafted, reviewed and edited the manuscript. All authors read and approved the final version of manuscript.

Ethics approval and consent to participate

All animal experimental procedures were approved by the Ethics Committee for Laboratory Animals of the Nanjing Medical University (approval no. 20181207). The date of the original ethics approval was prior to 2020.

Patient consent for publication

Not applicable.

Competing interests

The authors declare that they have no competing interests.

References

1. Lee R, Wong TY and Sabanayagam C: Epidemiology of diabetic retinopathy, diabetic macular edema and related vision loss. Eye Vis (Lond) 2: 17, 2015.
2. Sabanayagam C, Banu R, Chee ML, Lee R, Wang YX, Tan G, Jonas JB, Lamoureux EL, Cheng CY, Klein BEK, *et al*: Incidence and progression of diabetic retinopathy: A systematic review. Lancet Diabetes Endocrinol 7: 140-149, 2019.
3. Cheung N, Mitchell P and Wong TY: Diabetic retinopathy. Lancet 376: 124-136, 2010.
4. Lechner J, O'Leary OE and Stitt AW: The pathology associated with diabetic retinopathy. Vision Res 139: 7-14, 2017.
5. Xu Y, Cui K, Li J, Tang X, Lin J, Lu X, Huang R, Yang B, Shi Y, Ye D, *et al*: Melatonin attenuates choroidal neovascularization by regulating macrophage/microglia polarization via inhibition of RhoA/ROCK signaling pathway. J Pineal Res 69: e12660, 2020.
6. Lynch SK and Abràmoff MD: Diabetic retinopathy is a neurodegenerative disorder. Vision Res 139: 101-107, 2017.
7. Dehdashtian E, Mehrzadi S, Yousefi B, Hosseinzadeh A, Reiter RJ, Safa M, Ghaznavi H and Naseripour M: Diabetic retinopathy pathogenesis and the ameliorating effects of melatonin; involvement of autophagy, inflammation and oxidative stress. Life Sci 193: 20-33, 2018.
8. Coughlin BA, Feenstra DJ and Mohr S: Müller cells and diabetic retinopathy. Vision Res 139: 93-100, 2017.
9. Shen W, Fruttiger M, Zhu L, Chung SH, Barnett NL, Kirk JK, Lee S, Coorey NJ, Killingsworth M, Sherman LS, *et al*: Conditional Müllercell ablation causes independent neuronal and vascular pathologies in a novel transgenic model. J Neurosci 32: 15715-15727, 2012.
10. Zong H, Ward M, Madden A, Yong PH, Limb GA, Curtis TM and Stitt AW: Hyperglycaemia-induced pro-inflammatory responses by retinal Müller glia are regulated by the receptor for advanced glycation end-products (RAGE). Diabetologia 53: 2656-2666, 2010.

11. McDowell RE, Barabas P, Augustine J, Chevallier O, McCarron P, Chen M, McGeown JG and Curtis TM: Müller glial dysfunction during diabetic retinopathy in rats is reduced by the acrolein-scavenging drug, 2-hydrazino-4,6-dimethylpyrimidine. Diabetologia 61: 2654-2667, 2018.

12. Wu S, Zhu X, Guo B, Zheng T, Ren J, Zeng W, Chen X and Ke M: Unfolded Protein Response Pathways Correlatively Modulate Endoplasmic Reticulum Stress Responses in Rat Retinal Müller Cells. J Ophthalmol 2019: 9028483, 2019.

13. Tien T, Zhang J, Muto T, Kim D, Sarthy VP and Roy S: High Glucose Induces Mitochondrial Dysfunction in Retinal Müller Cells: Implications for Diabetic Retinopathy. Invest Ophthalmol Vis Sci 58: 2915-2921, 2017.

14. Rübsam A, Parikh S and Fort PE: Role of Inflammation in Diabetic Retinopathy. Int J Mol Sci 19: 19, 2018.

15. Ito S and Nagata K: Biology of Hsp47 (Serpin H1), a collagen-specific molecular chaperone. Semin Cell Dev Biol 62: 142-151, 2017.

16. Zhang X, Yang JJ, Kim YS, Kim KY, Ahn WS and Yang S: An 8-gene signature, including methylated and down-regulated glutathione peroxidase 3, of gastric cancer. Int J Oncol 36: 405-414, 2010.

17. Poschmann G, Sitek B, Sipos B, Ulrich A, Wiese S, Stephan C, Warscheid B, Klöppel G, Vander Borght A, Ramaekers FC, *et al*: Identification of proteomic differences between squamous cell carcinoma of the lung and bronchial epithelium. Mol Cell Proteomics 8: 1105-1116, 2009.

18. Zhu J, Xiong G, Fu H, Evers BM, Zhou BP and Xu R: Chaperone Hsp47 Drives Malignant Growth and Invasion by Modulating an ECM Gene Network. Cancer Res 75: 1580-1591, 2015.

19. Sepulveda D, Rojas-Rivera D, Rodríguez DA, Groenendyk J, Köhler A, Lebeaupin C, Ito S, Urra H, Carreras-Sureda A, Hazari Y, *et al*: Interactome Screening Identifies the ER Luminal Chaperone Hsp47 as a Regulator of the Unfolded Protein Response Transducer IRE1α. Mol Cell 69: 238-252.e7, 2018.

20. Yoneda A, Sakai-Sawada K, Minomi K and Tamura Y: Heat Shock Protein 47 Maintains Cancer Cell Growth by Inhibiting the Unfolded Protein Response Transducer IRE1α. Mol Cancer Res 18: 847-858, 2020.

21. Xu X, Qimuge A, Wang H, Xing C, Gu Y, Liu S, Xu H, Hu M and Song L: IRE1α/XBP1s branch of UPR links HIF1α activation to mediate ANGII-dependent endothelial dysfunction under particulate matter (PM) 2.5 exposure. Sci Rep 7: 13507, 2017.

22. Chen X, Iliopoulos D, Zhang Q, Tang Q, Greenblatt MB, Hatziapostolou M, Lim E, Tam WL, Ni M, Chen Y, *et al*: XBP1 promotes triple-negative breast cancer by controlling the HIF1α pathway. Nature 508: 103-107, 2014.

23. Yang J, Chen C, McLaughlin T, Wang Y, Le YZ, Wang JJ and Zhang SX: Loss of X-box binding protein 1 in Müller cells augments retinal inflammation in a mouse model of diabetes. Diabetologia 62: 531-543, 2019.

24. Liu X, Tang L and Liu Y: Mouse Müller Cell Isolation and Culture. Bio Protoc 7: e2429, 2017.

25. Pereiro X, Ruzafa N, Acera A, Urcola A and Vecino E: Optimization of a Method to Isolate and Culture Adult Porcine, Rats and Mice Müller Glia in Order to Study Retinal Diseases. Front Cell Neurosci 14: 7, 2020.

26. Livak KJ and Schmittgen TD: Analysis of relative gene expression data using real-time quantitative PCR and the 2(-Delta Delta C(T)) Method. Methods 25: 402-408, 2001.

27. Zhong Y, Li J, Chen Y, Wang JJ, Ratan R and Zhang SX: Activation of endoplasmic reticulum stress by hyperglycemia is essential for Müller cell-derived inflammatory cytokine production in diabetes. Diabetes 61: 492-504, 2012.

28. Semeraro F, Cancarini A, dell'Omo R, Rezzola S, Romano MR and Costagliola C: Diabetic Retinopathy: Vascular and Inflammatory Disease. J Diabetes Res 2015: 582060, 2015.

29. Xu Z, Wei Y, Gong J, Cho H, Park JK, Sung ER, Huang H, Wu L, Eberhart C, Handa JT, *et al*: NRF2 plays a protective role in diabetic retinopathy in mice. Diabetologia 57: 204-213, 2014.

30. Rodrigues M, Xin X, Jee K, Babapoor-Farrokhran S, Kashiwabuchi F, Ma T, Bhutto I, Hassan SJ, Daoud Y, Baranano D, *et al*: VEGF secreted by hypoxic Müller cells induces MMP-2 expression and activity in endothelial cells to promote retinal neovascularization in proliferative diabetic retinopathy. Diabetes 62: 3863-3873, 2013.

31. Lieth E, LaNoue KF, Antonetti DA and Ratz M; The Penn State Retina Research Group: Diabetes reduces glutamate oxidation and glutamine synthesis in the retina. Exp Eye Res 70: 723-730, 2000.

32. Bringmann A, Pannicke T, Uhlmann S, Kohen L, Wiedemann P and Reichenbach A: Membrane conductance of Müller glial cells in proliferative diabetic retinopathy. Can J Ophthalmol 37: 221-227, 2002.

33. Lai DW, Lin KH, Sheu WH, Lee MR, Chen CY, Lee WJ, Hung YW, Shen CC, Chung TJ, Liu SH, *et al*: TPL2 (Therapeutic Targeting Tumor Progression Locus-2)/ATF4 (Activating Transcription Factor-4)/SDF1α (Chemokine Stromal Cell-Derived Factor-α) Axis Suppresses Diabetic Retinopathy. Circ Res 121: e37-e52, 2017.

34. Kheitan S, Minuchehr Z and Soheili ZS: Exploring the cross talk between ER stress and inflammation in age-related macular degeneration. PLoS One 12: e0181667, 2017.

35. Zode GS, Sharma AB, Lin X, Searby CC, Bugge K, Kim GH, Clark AF and Sheffield VC: Ocular-specific ER stress reduction rescues glaucoma in murine glucocorticoid-induced glaucoma. J Clin Invest 124: 1956-1965, 2014.

36. Zhou Y, Bennett TM and Shiels A: Lens ER-stress response during cataract development in Mip-mutant mice. Biochim Biophys Acta 1862: 1433-1442, 2016.